

Kinetic ballooning instability for substorm onset and current disruption observed by AMPTE/CCE

C. Z. Cheng

Princeton Plasma Physics Laboratory, Princeton University, Princeton, NJ 08543

A. T. Y. Lui

Applied Physics Laboratory, Johns Hopkins University, Laurel, MD 20723

Abstract. A new interpretation of AMPTE/CCE observation of substorm onset and current disruption and the corresponding physical processes are presented. Toward the end of late growth phase the plasma β increases to ≥ 50 and a low frequency instability with a wave period of 50–75 sec is excited and grows to a large amplitude at the current disruption onset. At the onset, higher frequency instabilities are excited so that the plasma and electromagnetic field form a turbulent state. Plasma transport takes place to modify the ambient pressure profile so that the ambient magnetic field recovers from a tail-like geometry to a more dipole-like geometry. A new theory of kinetic ballooning instability (KBI) is proposed to explain the low frequency instability and the high β threshold ($\beta_c \geq 50$) observed by AMPTE/CCE. The stabilizing effect is mainly due to kinetic effects of trapped electrons and finite ion Larmor radii which give rise to a large parallel electric field and hence a parallel current that greatly enhances the stabilizing effect of field line tension. As a result β_c is greatly increased over the ideal MHD ballooning instability threshold by $\geq O(10^2 - 10^3)$. The wave-ion magnetic drift resonance effect produces a perturbed resonant ion velocity distribution centered at a duskward velocity roughly equal to the average ion magnetic drift velocity. This perturbed ion distribution explains the enhanced duskward ion flux during the explosive growth phase and can excite higher frequency instabilities (such as the cross-field current instability).

Introduction

A critical process in the previously established view of the substorm onset and current disruption based on the observation of the AMPTE/CCE spacecraft is the explosive growth phase (which lasts ~ 30 sec) at the approach of current disruption onset [Ohtani *et al.*, 1992]. During the explosive growth phase a large upsurge in the duskward ion flux is found near the local midnight sector which could lead to the excitation of the cross-field current instability (CCI) during the current disruption phase [Lui, 1996]. In this paper a new scenario of the AMPTE/CCE observation of substorm explosive growth phase, onset and current disruption is presented. In the late growth phase the plasma β is typically ~ 20 at ~ 10 minutes prior to the current disruption onset. At ~ 2 minutes before the onset β increases to ≥ 50 , the pressure becomes isotropic [Lui *et al.*, 1992], and a low frequency instability with a wave period of $\sim 50 - 75$ sec is

excited and grows exponentially to a large amplitude with $\delta B/B \geq 0.5$ at the onset. The half wave period of the instability before the onset corresponds to the explosive growth phase with an enhanced duskward ion flux. At the onset higher frequency instabilities (with wave periods of 15 sec, 10, sec, 5 sec, etc.) are excited and they combine with the low-frequency instability to form a strong turbulence state for $\sim 4 - 5$ minutes. During the turbulent state anomalously fast plasma transport takes place to modify the average pressure profile so that the ambient magnetic field relaxes from a tail-like geometry to a more dipole-like geometry.

Two key issues need to be resolved to further understand the physical processes of current disruption and subsequent magnetic field dipolarization: (1) the excitation mechanism and the high plasma β threshold (≥ 50) of the low frequency instability that underlines the explosive growth phase; (2) the physical mechanism of the enhanced duskward ion flux that occurs only during the explosive growth phase and leads to excitation of higher frequency instabilities. To understand these two key issues, we have developed a new theory of kinetic ballooning instability (KBI), which results from the release of free energy of nonuniform pressure with gradient in the same direction as the magnetic field curvature. Analogous to the expansion of a balloon due to higher inner air pressure around weak surface tension spot, the ballooning instability will relax higher plasma pressure and hence the magnetic field across the large field line curvature surface toward the weaker pressure direction. Previously the ideal MHD ballooning instability has been proposed to explain the current disruption and explosive growth phase [Roux *et al.*, 1991; Liu, 1997; Voronkov *et al.*, 1997]. The ideal MHD ballooning mode theory would predict a low critical β ($\beta_c \leq 1$) for instability, which is contrary to the high β values (≥ 20) observed by AMPTE/CCE throughout the late growth phase. In this paper we show that kinetic effects such as trapped particle dynamics, finite ion Larmor radii (FLR) and wave-particle resonances are important in determining the stability of KBI and we are able to answer these two key issues of substorm onset and current disruption. In particular, we show that the KBI theory properly explains the wave frequency, growth rate and high β_c (≥ 50) of the low frequency instability as well as the enhanced duskward ion flux during the explosive growth phase observed by the AMPTE/CCE.

Low-Frequency Perturbation

Evidence for a low-frequency perturbation occurring prior to current disruption onset can be found in detailed examination of magnetic field during current disruption events. Figure 1 shows the result of such an analysis. Magnetic field measurements from AMPTE/CCE on August 30, 1986 were

Copyright 1998 by the American Geophysical Union.

Paper number GRL-1998900093.
0094-8276/98/GRL-1998900093\$05.00

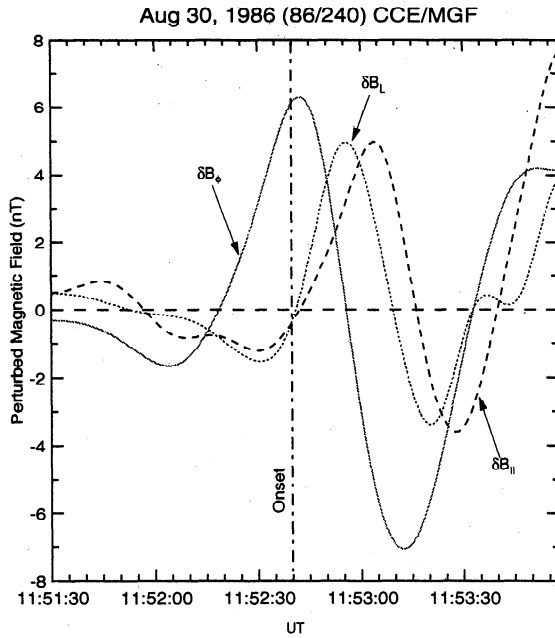


Figure 1. Three components of the low frequency perturbed magnetic field.

studied. The satellite was in the midnight local time sector, MLT = 23.5, at a radial distance of $\approx 8R_E$. The current disruption onset time is at 11:52:40 UT [Lui et al., 1992; Ohtani et al., 1995]. To extract the low frequency components of the fluctuations, we employed successive smoothing of the original data with normalized binomial coefficients as previously used in Lui and Najmi [1997]. The derived magnetic field perturbations in the cylindrical (V , D , H) components magnetic field coordinate system to give δB_L , δB_ϕ , and δB_\parallel , where positive δB_ϕ is pointing eastward, positive δB_\parallel is along the mean magnetic field direction and positive δB_L is in the third right-handed orthogonal direction. From Figure 1 the real frequency of the low-frequency perturbation is ~ 0.1 Hz (compared with proton cyclotron frequency of about 1 Hz) and the growth rate is about 0.2 of the real frequency. Note that the unstable perturbation begins quite early at $\sim 11:51:30$ UT, ~ 1.5 min before the onset of current disruption. We have further confirmed that before onset the perturbation is in a linear growth phase because the relative wave phases of the three magnetic field components are in agreement with the wave structure of the linear ballooning instability [Cheng and Qian, 1994]. It is interesting to note that there is almost no magnetic field fluctuation before the low frequency instability was observed. Although not shown here, a low frequency perturbation similar to that shown here has also been found in a June 1, 1985 current disruption event [Lui et al., 1992] which we have examined.

The 30 sec period (11:52:10 – 11:52:40UT) of the low frequency instability (with amplitude reaching $\delta B/B \geq 0.5$) just before the current disruption onset was previously called “explosive growth phase” [Ohtani et al., 1992] which is accompanied by a large increase of the duskward ion flux centered at ~ 500 km/s (below the ion thermal velocity of ≈ 1000 km/s) [Lui, 1996]. This enhanced cross-tail ion drift population is responsible for exciting higher frequency instabilities which together with the low frequency instability last throughout the current disruption phase to form a strong turbulence. Note that the duskward ion flux enhancement lasts only in the explosive growth phase.

During the late growth phase the plasma pressure in the midnight sector at approximately $8R_E$ [Lui et al., 1992] increases $\leq 20\%$ from ~ 10 minutes prior to the current disruption onset to the time the low frequency instability is excited. The corresponding plasma β increases from ~ 20 to ≥ 50 also due to the reduction of the magnetic field intensity. The pressure increase may be due to Fermi acceleration process [Ganguli et al., 1995] or plasma convection [Erickson, 1992]. This pressure change leads to further thinning of the plasma sheet. Although there is no observational determination of the pressure profile during the late growth phase, it is reasonable to expect that the plasma pressure decreases monotonically with increasing radial distance.

Kinetic Ballooning Instability

To understand the observed low-frequency instability we consider KBI. Based on the AMPTE/CCE observation of particle data [Lui et al., 1992; Lui, 1996], the average electron energy at the end of the growth phase is about 5 keV and the average ion energy is about 10 keV. The particle velocity distribution function does not have appreciable bulk drift and the plasma pressure becomes isotropic in the late growth phase at a few minutes before the onset. With this information we consider KBI perturbations with the orderings: $k_\perp \rho_i \sim O(1)$ and $k_\parallel \ll k_\perp$ and $v_{the} > (\omega/k_\parallel) > v_{thi}$ [Cheng, 1982b, 1982a; Cheng et al., 1995], where ρ_i is the ion gyroradius, k is the wave number, and \parallel and \perp represent parallel and perpendicular components to the equilibrium magnetic field. With these orderings the following kinetic effects must be considered: trapped electron dynamics, ion FLR effect and wave-ion magnetic drift resonance.

We shall derive the KBI eigenmode equation by obtaining approximate solutions of the perturbed particle distributions based on the gyrokinetic formulation with the assumption that both electrons and ions have local Maxwellian equilibrium distribution functions. The detailed derivation can be found in our previous papers [Cheng, 1982a; Cheng et al., 1995]. Including full FLR effects we express the perturbed particle distribution function in the rationalized MKS unit as $\delta f = (q/M)(\partial F/\partial \mathcal{E})[(\omega_*^T/\omega)\Phi - (1 - \omega_*^T/\omega)(1 - J_0 e^{i\delta L})\Phi] + g e^{i\delta L}$, where q is the particle charge, M is the particle mass, $\omega_*^T = \mathbf{B} \times \mathbf{k}_\perp \cdot \nabla F / (B\omega_c \partial F/\partial \mathcal{E})$, $\delta L = \mathbf{k} \times \mathbf{v} \cdot \mathbf{B}/\omega_c B$, J_l is the l -th order Bessel function of the argument $k_\perp v_\perp/\omega_c$, $\omega_c = qB/M$ is the cyclotron frequency, Φ is the perturbed electrostatic potential, the guiding center particle equilibrium distribution F is a function of L -shell and particle energy \mathcal{E} , and g is the nonadiabatic part of the perturbed distribution function. Based on the WKB-ballooning formalism the gyrokinetic equation [Catto et al., 1981] in the low frequency ($\omega \ll \omega_c$) limit is given by

$$(\omega - \omega_d + i\mathbf{v}_\parallel \cdot \nabla_\parallel)g = -\frac{q}{M} \frac{\partial F}{\partial \mathcal{E}} \left(1 - \frac{\omega_*^T}{\omega}\right) \times \left[(\omega_d \Phi - i\mathbf{v}_\parallel \cdot \nabla_\parallel \Psi) J_0 + \frac{v\omega_\perp}{k_\perp} J_1 \delta B_\parallel\right], \quad (1)$$

where Ψ is the parallel perturbed electric field potential with $\mathbf{E}_\parallel = -\nabla_\parallel \Psi$, δB_\parallel is the parallel perturbed magnetic field, $\omega_d = \mathbf{k}_\perp \cdot \mathbf{v}_d$ is the magnetic drift frequency, $\mathbf{v}_d = (\mathbf{B}/B\omega_c) \times (v_\perp^2 \boldsymbol{\kappa} + \mu \nabla B)$ is the magnetic drift velocity, and $\boldsymbol{\kappa}$ is the magnetic field curvature. Note that the vector potential, defined by $\mathbf{A} = \mathbf{A}_\parallel - i\delta \mathbf{B}_\perp \times \mathbf{k}_\perp/k_\perp^2$, is related to Φ and Ψ by $\omega \mathbf{A}_\parallel = -i\nabla_\parallel(\Phi - \Psi)$. We note that the gyrokinetic formulation is still valid for ion Larmor radii on the order of equilibrium scale length if the ion magnetic drift frequency is replaced with the pitch angle average value to account for

the non-conservation of the magnetic moment [Hurricane *et al.*, 1994].

For electrons we shall neglect FLR effects and consider $|v_{\parallel} \nabla_{\parallel}| \gg \omega, \omega_{de}$. Trapped and untrapped electrons have very different parallel dynamics. The untrapped electron dynamics is mainly determined by its fast parallel transit motion, and to the lowest order in $(\omega/|v_{\parallel} \nabla_{\parallel}|)$ the perturbed untrapped electron density is given by

$$\delta n_{eu} = \frac{eN_{eu}}{T_e} \left[\frac{\omega_{*e}}{\omega} \Phi + \left(1 - \frac{\omega_{*e}}{\omega}\right) \Psi \right], \quad (2)$$

where $\omega_{*e} = \mathbf{B} \times \nabla N_e \cdot \mathbf{k}_{\perp} / (B\omega_{ce}N_e)$ is the electron diamagnetic drift frequency, $N_{eu}/N_e = 1 - [1 - B(s)/B_i]^{1/2}$ is the untrapped electron fraction at the location s , B_i is B at the ionosphere. Near the equator $N_{eu}/N_e \simeq B(s)/2B_i \ll 1$. The trapped electron dynamics is mainly determined by its fast bounce motion and to the lowest order in (ω/ω_{be}) the perturbed trapped electron density is

$$\delta n_{et} \simeq \frac{eN_{et}}{T_e} \left[\frac{\omega_{*e}}{\omega} \Phi + \left(1 - \frac{\omega_{*e}}{\omega}\right) \Delta \Psi \right] + \delta \hat{n}_{et}, \quad (3)$$

where $N_{et}/N_e = [1 - B(s)/B_i]^{1/2}$ is the fraction of trapped electrons,

$$\Delta = \int_{tr} d^3v (F_e/N_{et}) \left[1 - \frac{\langle (\omega - \omega_{de}) \Psi \rangle}{\langle \omega - \omega_{de} \rangle} \right], \quad (4)$$

$\delta \hat{n}_{et} = - \int_{tr} d^3v (eF_e/T_e) [(\omega - \omega_{*e}^T)/(\omega - \langle \omega_{de} \rangle)] \times \langle (\omega_{de}/\omega) \Phi + v_{\perp}^2 \delta B_{\parallel} / 2\omega_{ce} \rangle$, and $\langle \omega_{de} \rangle$ is the trapped particle orbit average of ω_{de} . Note that $\Delta \ll 1$ near the equator.

To obtain the nonadiabatic perturbed ion distribution function we assume that $\omega, \omega_{di} \gg |v_{\parallel} \nabla_{\parallel}|$, and we have

$$g_i \simeq \frac{eF_i}{T_i} \frac{\omega - \omega_{*i}^T}{\omega - \omega_{di}} \left(\frac{\omega_{di} J_0 \Phi}{\omega} + \frac{v_{\perp} J_1 \delta B_{\parallel}}{k_{\perp}} \right). \quad (5)$$

The ion dynamics is mainly determined by its perpendicular motion and the perturbed ion density is given by

$$\delta n_i = - \frac{eN_i}{T_i} \left[\frac{\omega_{*i}}{\omega} \Phi + \left(1 - \frac{\omega_{*i}}{\omega}\right) (1 - \Gamma) \Phi \right] + \delta \hat{n}_i, \quad (6)$$

where $\omega_{*i} = \mathbf{B} \times \nabla N_i \cdot \mathbf{k}_{\perp} / (B\omega_{ci}N_i)$, $\omega_{*pi} = \mathbf{B} \times \nabla P_i \cdot \mathbf{k}_{\perp} / (B\omega_{ci}P_i)$, $\Gamma(b_i) = I_0(b_i) \exp(-b_i)$, $b_i = k_{\perp}^2 T_i / M_i \omega_{ci}^2 = k_{\perp}^2 \rho_i^2 / 2$, I_0 is the modified Bessel function of the zeroth order, and $\delta \hat{n}_i = \int d^3v g_i J_0$.

From the charge quasi-neutrality condition we obtain the parallel electric field potential

$$\left(\frac{N_{eu} + N_{et} \Delta}{N_e} \right) \Psi = - \frac{T_e}{T_i} \frac{\omega - \omega_{*pi}}{\omega - \omega_{*e}} (1 - \Gamma) \Phi + \frac{T_e}{eN_e} (\delta \hat{n}_i - \delta \hat{n}_{et}) \quad (7)$$

In comparison with the limit without trapped electron effects, the parallel electric field is enhanced by $N_e/(N_{eu} + N_{et} \Delta)$ which is much larger than unity near the equator for $b_i \sim O(1)$. From the parallel Ampere's law the perturbed parallel current is given by $\delta J_{\parallel} \simeq i \nabla_{\perp}^2 \nabla_{\parallel} (\Phi - \Psi) / \omega$, which represents the enhancement of stabilizing field line tension due to effects of trapped electrons and ion FLR.

Following the derivation presented in the paper by Cheng *et al.* [1995], we obtain from the parallel Ampere's law

$$\mathbf{B} \cdot \nabla \left[\frac{k_{\perp}^2}{B^2} \mathbf{B} \cdot \nabla (\Phi - \Psi) \right] + \frac{\omega(\omega - \omega_{*pi})}{V_A^2} \frac{1 - \Gamma(b_i)}{\rho_i^2/2} \Phi + \frac{\mathbf{B} \times \boldsymbol{\kappa} \cdot \mathbf{k}_{\perp}}{B^2} \left(\frac{2\mathbf{B} \times \nabla P \cdot \mathbf{k}_{\perp}}{B^2} \Phi - \omega \sum_j \delta \hat{p}_j \right) = 0 \quad (8)$$

where $V_A = B/(n_i M_i)^{1/2}$ is the Alfvén speed, and the non-

adiabatic perturbed pressures for each particle species are given by $\delta \hat{p}_j = M_j \int d^3v [(1 - \omega_{*j}^T/\omega)(1 - J_0^2) \Phi + g_j J_0] (v_{\perp}^2/2 + v_{\parallel}^2)$. Note that the relation $\mathbf{B} \cdot \delta \mathbf{B} + \delta P_{\perp} \simeq 0$ is used for low frequency instabilities with $\omega \ll k_{\perp} V_A$ [Cheng, 1991; Cheng and Qian, 1994; Cheng *et al.*, 1995].

Equations (7) and (8) form a coupled set of KBI eigenmode equations for solving Φ and Ψ along the field lines and the eigenvalue ω . We also need to obtain the nonadiabatic contributions of perturbed densities, $\delta \hat{n}_{et}$ and $\delta \hat{n}_i$, and perturbed particle pressures, $\delta \hat{p}_{\parallel}$ and $\delta \hat{p}_{\perp}$. The eigenmode equations include kinetic effects of trapped electron dynamics, parallel electric field, full ion FLR, and wave-particle resonances. Considering the ordering $\omega \gg \omega_{de}, \omega_{di}$, the nonadiabatic density and pressure responses in Eqs. (7) and (8), can be neglected and the local dispersion relation for KBI is approximately given by

$$\frac{\omega(\omega - \omega_{*pi})}{(1 + b_i)V_A^2} \simeq S k_{\parallel}^2 - \frac{2\boldsymbol{\kappa} \cdot \nabla P}{B^2}, \quad (9)$$

where $S = 1 + (b_i/(1 + b_i))N_e T_e / (N_{eu} + N_{et} \Delta) T_i \gg 1$, and the Padé approximation $1 - \Gamma \simeq b_i/(1 + b_i)$ is used. The real frequency of KBI is $\omega_r = \omega_{*pi}/2$ and the critical β is

$$\beta_c \simeq S \beta_c^{MHD} + \frac{\omega_{*pi}^2 R_c L_p}{4(1 + b_i)V_A^2}, \quad (10)$$

where R_c is the radius of the magnetic field curvature and L_p is the pressure gradient scale length, and $\beta_c^{MHD} = k_{\parallel}^2 R_c L_p$ is the ideal MHD β threshold. It has previously been calculated that $\beta_c^{MHD} \simeq 0.2$ for a dipole field with $L_p = 1R_E$ at $L = 8$ [Cheng and Qian, 1994]. For a more tail-like field we expect that β_c^{MHD} will be even smaller. Note that based on the AMPTE/CCE observation of $B = 10$ nT, $T_e/T_i = 0.5, b_i = 0.5$, we have $S \simeq 10^2 - 10^3$, then $\beta_c \geq O(10^2) \beta_c^{MHD} \sim O(10)$. Assuming that $L_p = 0.5R_E$ and $k_y \rho_i = 1$ the KBI real frequency is $\omega_r \simeq 0.2 s^{-1}$ and from past calculations [Cheng, 1982a, 1982b] the growth rate is usually about $0.1\omega_r$ for β of 5–10% higher than β_c . These results are consistent with the AMPTE/CCE observation.

If $\omega \sim \omega_{di}$, the wave-ion magnetic drift resonance can modify the growth rate and β_c . To fully evaluate the effect of the magnetic drift resonance, we retain ion nonadiabatic responses in the perturbed density and pressures. Numerical studies of KBI have been performed for tokamaks previously [Cheng, 1982b, 1982a] and the results indicated that the magnetic drift resonance effect reduces β_c by 20% at most and the real frequency of KBI will increase to ω_{*pi} at β_c . We expect the results for the magnetosphere will be qualitatively similar to the tokamak case and the numerical solutions will be presented in the future.

One consequence of the wave-ion magnetic drift resonance is that the perturbed ion distribution has a $(\omega - \omega_{di})$ resonance denominator. Because $\omega_r \simeq \omega_{*pi}/2$, the magnetic drift resonance will occur at $v_{di} = T_i \mathbf{B} \times \nabla P_i / (2eP_i B^2) \simeq v_{thi} \rho_i / 2L_{pi}$, where L_{pi} is the ion pressure gradient scale length. Thus, $|v_{di}| \sim 0.5v_{thi}$ for $\rho_i \sim L_{pi}$. As KBI grows to a large amplitude with $\delta B/B \geq 0.5$, the resulting change in ion velocity distribution gives rise to a positive slope near the duskward resonant ion magnetic drift velocity, and provides an additional free energy source for exciting higher frequency instabilities. Note that because the perturbed distribution oscillates with KBI, the duskward ion flux should be enhanced only in a one-half wave period and should be reduced in the other half wave period. These features are in qualitative agreement with the AMPTE/CCE measurement of ion flux.

Summary and Discussion

In this paper we have identified a new scenario and physical processes of substorm explosive growth phase, onset and current disruption observed by AMPTE/CCE. We have found a low-frequency instability with a wave period of about 50 – 75 sec excited at approximately 2 minutes before the current disruption onset, and we have interpreted it as the kinetic ballooning instability (KBI). The β threshold (≥ 50) for exciting KBI is at least 10^2 larger than that based on the ideal MHD theory because of the kinetic effects of trapped electron dynamics and finite ion Larmor radii which give rise to a large parallel electric field and hence a parallel current that greatly enhances the stabilizing effect of field line tension. With KBI we are able to explain the enhanced duskward ion flux which occurs only during the explosive growth phase (≈ 30 sec) and can excite higher frequency instabilities such as CCI. Thus, our new substorm scenario emphasizes KBI which can naturally account for the features of the explosive growth phase and the initiation of current disruption through a combination of KBI and higher frequency instabilities such as CCI.

The physical processes presented in the paper has not directly made use of the concept of ion chaotic motion and Fermi acceleration [Ganguli *et al.*, 1995] related to the thinning of the plasma sheet. These processes can have impact on the ion distribution function during the late growth phase. As the plasma sheet thins to a scale length of ion gyroradius, the ion energy will increase due to Fermi acceleration process which can contribute to destabilize KBI. The ion motion can become chaotic due to non-conservation of particle magnetic moment (μ) on a time scale of several ion gyro-periods and the ion pressure becomes isotropic. The change of μ also leads to a change in ion drift velocity. However, because the KBI parallel wave phase velocity is larger than ion thermal velocity and the wave frequency is larger than typical ion magnetic drift frequency, the stochastic change of ion magnetic drift frequency does not have a primary effect on the KBI stability. The primary stabilization effect remains to be the trapped electron dynamics and ion FLR that enhance the parallel electric field and the parallel current which provides a large field line tension to increase β_c .

Acknowledgments. This work is supported by the NSF Grants No. ATM-9523331 and No. ATM- 9622080 and the DoE Contract No. DE-AC02-76-CHO3073.

References

- Catto, P. J., W. M. Tang, and D. E. Baldwin, Generalized gyrokinetics, *Plasma Phys.*, *23*, 639, 1981.
 Cheng, C. Z., High- n collisionless ballooning modes in axisymmetric toroidal plasmas, *Nucl. Fusion*, *22*, 773, 1982a.

- Cheng, C. Z., Kinetic theory of collisionless ballooning modes, *Phys. Fluids*, *25*, 1020, 1982b.
 Cheng, C. Z., A kinetic-magnetohydrodynamic model for low-frequency phenomena, *J. Geophys. Res.*, *96*, 21159, 1991.
 Cheng, C. Z., and Q. Qian, Theory of ballooning-mirror instabilities for anisotropic pressure plasmas in the magnetosphere, *J. Geophys. Res.*, *99*, 11193, 1994.
 Cheng, C. Z., N. N. Gorelenkov, and C. T. Hsu, Fast particle destabilization of TAE modes, *Nucl. Fusion*, *35*, 1639, 1995.
 Erickson, G. M., A quasi-static magnetospheric convection model in two-dimensions, *J. Geophys. Res.*, *97*, 6505, 1992.
 Ganguli, G., P. J. Palmadesso, J. Fedder, and A. T. Y. Lui, Role of Fermi acceleration in explosive enhancement of cross-tail current in late substorm growth phase, *Geophys. Res. Lett.*, *22*, 2405, 1995.
 Hurricane, O. A., R. Pellat, and F. V. Coroniti, The kinetic response of a stochastic plasma to low frequency perturbations, *Geophys. Res. Lett.*, *21*, 253, 1994.
 Liu, W. W., Physics of the explosive growth phase: Ballooning instabilities revisited, *J. Geophys. Res.*, *102*, 4927, 1997.
 Lui, A. T. Y., Current disruption in the Earth's magnetosphere: Observations and models, *J. Geophys. Res.*, *101*, 13067, 1996.
 Lui, A. T. Y., and A.-H. Najmi, Time-frequency decomposition of signals in a current disruption event, *Geophys. Res. Lett.*, *24*, 3157, 1997.
 Lui, A. T. Y., et al., Current disruptions in the near-Earth neutral sheet region, *J. Geophys. Res.*, *97*, 1461, 1992.
 Ohtani, S., K. Takahashi, L. Zanetti, T. A. Potemra, R. W. McEntire, and T. Iijima, Initial signatures of magnetic field and energetic particle fluxes at tail reconfiguration: Explosive growth phase, *J. Geophys. Res.*, *97*, 19311, 1992.
 Ohtani, S., T. Higuchi, A. T. Y. Lui, and K. Takahashi, Magnetic fluctuations associated with tail current disruption: Fractal analysis, *J. Geophys. Res.*, *100*, 19135, 1995.
 Roux, A., S. Perraut, A. Moranc, P. Robert, A. Korth, G. Kremser, A. Pederson, R. Pellinen, and Z. Y. Pu, Plasma sheet instability related to the westward traveling surge, *J. Geophys. Res.*, *96*, 17697, 1991.
 Voronkov, L., R. Rankin, P. Frycz, V. T. Tikonchuk, and J. C. Samson, Coupling of shear flow and pressure gradient instabilities, *J. Geophys. Res.*, *102*, 9639, 1997.

C. Z. Cheng, Princeton Plasma Physics Laboratory, Princeton University, P. O. Box 451, Princeton, NJ 08543;
 A. T. Y. Lui, Applied Physics Laboratory, Johns Hopkins University, Laurel, MD 20723

(received May 8, 1998; revised August 21, 1998;
 accepted September 15, 1998.)